







# Design of a White Cement-Based Concrete Fabric for Architectural Applications

Serdal Ünal<sup>1\*</sup> , Kerem Aybar<sup>2</sup> , Ömer Karagöz<sup>1</sup> , Mehmet Canbaz<sup>1</sup> 

<sup>1</sup>Department of Civil Engineering, Eskişehir Osmangazi University, Eskişehir, Türkiye

<sup>2</sup>Department of Metallurgical and Materials Engineering, Eskişehir Osmangazi University, Eskişehir, Türkiye

## Keywords

3D Textile  
Reinforced Concrete,  
Architectural  
Applications,  
Mechanical  
Performance,  
White Cement  
Composite.

## Abstract

Modern architectural designs demand materials that are both aesthetically flexible and functionally lightweight and durable. To address this need, white cement-based, 3D textile-reinforced composites with waterproof membranes were developed. The aim was to produce structural elements that are flexible, lightweight, water-resistant, and capable of retaining complex shapes. During fabrication, 3D textile pieces were placed into wooden molds, filled with white cement, and a waterproof membrane was applied to the surface. The specimens were tested for unit weight, flexural, and tensile properties at 7 and 28 days. The results demonstrated that the composites exhibited remarkably low unit weights ranging from 0.77 to 0.83 kg/dm<sup>3</sup>, high flexural strength of up to 16.32 MPa, and tensile elongation exceeding 30%. While initial crumbling of the cement matrix was observed during tensile testing, the textile reinforcement effectively preserved specimen integrity, limited crack propagation, and enhanced energy absorption. Consistent performance under both static and dynamic loading confirmed the material's ductility, shape adaptability, and robustness. These findings suggest that the composite is particularly suitable for architectural components requiring freeform geometries, flexibility, and portability. Additionally, its lightweight and water-resistant properties provide significant advantages for temporary or movable structures, as well as for integration with novel fabrication techniques such as 3D printing and modular construction systems.

## 1. Introduction

Textile reinforced concrete (TRC) has attracted increasing interest in the construction industry as an innovative composite material capable of producing lighter, more flexible, and durable structures compared to traditional concrete technology [1,2]. It is widely used in infrastructure projects, bridges, tunnels, water structures, and repair applications as an important alternative [3]. Thanks to its lightweight and high strength, it enables material and weight savings in both load-bearing and non-load-bearing elements, while its application flexibility allows the production of structural components with complex geometries [4]. In architectural fields, TRC is preferred in projects where aesthetics and functionality are equally important, facilitating the creation of freeform surfaces, curved, and organic facade elements [5]. Thus, architects gain more design freedom while optimizing both the visual and structural performance of buildings. Some architectural application of 3D textile concrete shown in Figure 1 and Figure 2.

Textile reinforced concretes are composite systems formed by integrating high-strength fibers—usually made of glass, carbon, aramid, or polymer-based materials—into a cementitious matrix [8]. These fibers significantly

\* Corresponding Author: serdalunall@gmail.com

Received: August 15, 2025, Accepted: September 14, 2025

reduce the brittle fracture behavior of concrete, increasing its ductility [9]. Key properties of TRC include high tensile strength, enhanced crack control, low weight, high energy absorption, and long service life [10]. Moreover, the textile's geometric structure and orientation directly affect the mechanical performance of the composite; 3D textiles provide more homogeneous and multidirectional strength due to fiber distribution in different directions [11]. Additionally, the resistance of these materials to water and environmental degradation makes them particularly attractive for outdoor and water-related applications. Studies conducted in the last few years have investigated aspects such as the influence of textile geometry on crack distribution and energy absorption, the use of eco-friendly binders in TRC composites, and the integration of digital fabrication techniques such as 3D printing [12]. Moreover, the incorporation of advanced textile materials has been reported to enhance both tensile ductility and long-term durability under environmental effects including freeze–thaw cycles, moisture, and UV exposure [13, 14]. These recent developments highlight that TRC research is evolving from purely structural considerations toward multifunctional and design-oriented solutions. In this context, the current study contributes by combining white cement, 3D textile reinforcement, and a waterproof membrane, offering a novel approach that directly addresses both the mechanical performance and aesthetic requirements of architectural applications.



**Figure 1.** Examples of street furniture produced using 3D textile concrete [6,7].



**Figure 2.** Example of tiny houses constructed with 3D textile concrete [15].

In recent years, sustainability and environmental awareness have become key focus areas in the field of construction materials [16]. White cement-based, lightweight, and durable textile reinforced composites are considered eco-friendly solutions due to their lower carbon footprint during production and contribution to energy savings by reducing the weight of structural elements [17]. Additionally, the integration of 3D textile

reinforcement and waterproof membranes not only enhances the mechanical performance of these materials but also offers great potential for architectural applications compatible with modern manufacturing techniques such as digital fabrication and 3D printing. This enables achieving a balance between aesthetic flexibility and functional durability in architectural design, allowing the creation of unique and complex structural elements that are not feasible with conventional concrete. Although many studies exist on the mechanical performance and durability of textile reinforced concrete, comprehensive research on white cement-based, 3D textile-reinforced composites integrated with waterproof membranes for architectural applications is limited. Most studies focus on gray cement-based systems and lack investigation within the architectural context, where both aesthetic and functional requirements must be met. Furthermore, the effects of 3D textile reinforcement on material behavior and the role of waterproof membrane integration in mechanical performance have not been fully addressed. In contrast, the present study introduces a white cement-based composite system integrated with 3D textile reinforcement and a waterproof membrane, addressing both functional and aesthetic needs. This study evaluates the manufacturing process of architectural composites using white cement supported by mechanical tests, highlighting innovative contributions in designing flexible, lightweight, and water-resistant composites. Thus, it fills a significant gap in the literature by expanding material technology boundaries in architectural design and offering sustainable, performance-oriented solutions. Furthermore, the integration of a waterproof membrane distinguishes this study by contributing to durability and extending the applicability of the material to outdoor and moisture-sensitive architectural components.

## 2. Materials and Method

### 2.1. Materials

The White Portland cement CEM I 52.5N, characterized by the specific physical and chemical properties detailed in Table 1, was selected as the primary binder material for this study. This particular type of cement is renowned for its high early strength development and superior whiteness, which makes it especially suitable for architectural applications where aesthetics play a critical role. Moreover, its chemical composition and fineness contribute to enhanced durability and improved bonding with textile reinforcements, ensuring optimal performance of the composite material under various environmental and mechanical conditions. The use of white cement also distinguishes this research from conventional studies that typically employ gray cement, thus emphasizing the importance of color and visual impact in the development of innovative cementitious composites for architectural purposes.

**Table 1.** Properties of cements

SO <sub>3</sub> , %	3.38	Specific Surface, cm <sup>2</sup> /g	4700
LOI, %	2.61	Compressive strength, MPa	
Insoluble Residue, %	0.12	2 days	38
Initial Setting, min	100	28 days	60

The Eskişehir tap water, with the chemical and physical characteristics detailed in Table 2, was utilized as the mixing water in the preparation of the cementitious composites. The use of local tap water not only reflects practical and sustainable material sourcing but also ensures that the experimental conditions closely mimic real-world construction environments. The water quality parameters, including pH, hardness, and mineral content, were carefully considered to prevent any adverse effects on the hydration process and ultimate mechanical performance of the composite. By documenting the exact properties of the mixing water, the study enhances the reproducibility and reliability of the results, providing valuable reference data for future research and industrial applications in similar geographic regions.

**Table 2.** Properties of water

NO <sub>3</sub> , mg/l	11,2	Conductivity, $\mu$ S/cm	628
Ni, mg/l	5,07	Hardness, Fd <sup>0</sup>	30,11
K, mg/l	6,8	Turbidity, NTU	5
pH	7,35	Color, Co-Pt	20

The composite material employed in this study is reinforced with a 3D air-permeable fabric possessing a thickness of 6 mm, which plays a crucial role in enhancing both the mechanical performance and durability of the final product. This three-dimensional textile reinforcement facilitates improved bonding with the cementitious matrix, allowing for better stress distribution and crack control under various loading conditions. Additionally, its air-permeable structure contributes to optimal moisture regulation during curing, minimizing internal defects and enhancing long-term stability. The detailed physical and mechanical properties of this 3D fabric, including fiber composition, tensile strength, and porosity, are comprehensively listed in Table 3, providing essential data for understanding its contribution to the composite's behavior.

**Table 3.** Properties of fabric [18,19]

Components	Materials	Elongation, %	Tensile strength, MPa
Warp/Weft yarn MF	Polyethylene terephthalate multifilaments	9.2	443
Warp/weft yarn SF		6.1	731
Spacer yarn	Polyethylene terephthalate monofilaments	9.8	705
Warp, Weft	Volume content of spacer yarn % 2.91	Volume fraction of wrap-weft yarns, % 0.35	Volume fraction of matrix, 0.23

A waterproofing membrane with a thickness of 0.2 mm, reinforced with PVC on one side and fiber on the other, was employed to enhance the moisture resistance of the composite system. This dual reinforcement structure provides both mechanical strength and flexibility, ensuring a robust barrier against water ingress while maintaining compatibility with the cementitious matrix and textile layers. The membrane's physical, chemical, and mechanical properties, which are critical for its performance in preventing water penetration and contributing to the overall durability of the composite, are summarized in Table 4. Its integration within the composite plays a key role in extending the service life of architectural elements, especially in environments exposed to moisture or weathering.

**Table 4.** Properties of waterproof material

Components	Unit Area Weight, gr/m <sup>2</sup>	Tear Resistance, N
Oxidized bituminous waterproofing membrane	500	100

## 2.2.Method

In the design of fabric-reinforced concrete systems for architectural applications, the 3D textile material was prepared in different sizes suitable for mechanical testing. The textile was cut into dimensions of 30×30 cm for flexural tests and 30×10 cm for tensile tests. Considering the dual-surface structure of the 3D textile—one surface being porous and the other non-porous—the samples were placed in the molds with the porous face oriented upward. This placement strategy aimed to facilitate the penetration of cement into the textile and ensure an

effective bond with its three-dimensional structure. Subsequently, White Portland cement was distributed into the mold as shown in Figure 3, and a table vibrator was used to ensure that the cement fully filled the internal voids of the textile. This method contributed to a strong bond between the textile and the cement matrix, enabling the formation of a homogeneous composite structure. After casting, all specimens were removed from the mold after 24 hours and then cured under controlled conditions to ensure proper hydration and strength development. Specifically, the specimens were stored at room temperature until testing on days 7 and 28.



**Figure 3.** Cement casting into the 3D textile

The bituminous waterproofing membrane was cut into dimensions of 30×30 cm for the bending test and 30×10 cm for the tensile test. As shown in Figure 4, adhesive was applied to its surface.



**Figure 4.** Application of adhesive onto the waterproof membrane

After the adhesive was applied, the waterproofing membrane was carefully bonded onto the surface of the 3D textile, as illustrated in Figure 5. Ensuring a strong mechanical performance requires that the 3D textile be thoroughly saturated with white cement, allowing it to fill all internal voids effectively. However, it is important to control the amount of cement applied. Excessively spreading the dry binder over the surface may form a loose powder layer, which significantly reduces the bonding efficiency between the waterproofing membrane and the textile. Therefore, careful attention must be given to both cement placement and surface preparation to ensure optimal composite performance.

After the adhesion process was completed, the samples were carefully flipped over so that the water-permeable but cement-retaining surface of the 3D textile remained on top. Following this, as shown in Figure 6, water was applied to the surface to saturate the samples. This step ensured the controlled introduction of the necessary water for the hydration of the cement binder, while also preventing the cement particles on the surface from being washed away, thus preserving the integrity of the composite. This method contributed to the material hardening while maintaining its intended shape and enhancing its mechanical performance.



**Figure 5.** Adhesion of the waterproof membrane onto the surface of the 3D textile



**Figure 6.** Water immersion of cementitious 3D textile composites

The specimens, which were kept under standard curing conditions, were subjected to mechanical tests after 7 and 28 days of production. Bending tests were performed on samples with dimensions of  $30 \times 30 \times 0.6$  cm, as shown in Figure 7. These tests were conducted to evaluate the flexural behavior of the cement-based 3D textile composites and to observe the development of mechanical performance over time. The standardized curing process ensured proper hydration of the binder, contributing to consistent strength gain, while the 3D textile reinforcement played a crucial role in maintaining the structural integrity during bending. The results provided insights into the composite's suitability for architectural applications where flexibility and durability are essential.



**Figure 7.** Three-point bending test applied to the specimens

Tensile tests were conducted on samples with dimensions of  $30 \times 10 \times 0.6$  cm, as shown in Figure 8. In these tests, the top and bottom 8 cm sections of each sample were clamped, leaving a 14 cm free length in the middle for deformation observation. This configuration allowed for the analysis of elongation behavior and fracture characteristics within the effective gauge length. The aim was to evaluate the ductility and tensile integrity of the 3D textile-reinforced cementitious composite, as well as the contribution of the textile structure to strain

distribution and crack control during tensile loading. In this study, the term static tensile strength refers to tests carried out under a slow loading rate of 1 mm/min, ensuring gradual stress transfer and controlled deformation. The term dynamic tensile strength refers to tests performed at a higher loading rate of 30 mm/min, simulating rapid stress application. These loading rates were selected based on common practice in textile-reinforced concrete studies, enabling a consistent comparison of the material's performance under both sustained and sudden loading conditions.



**Figure 8.** Tensile test applied to the specimens

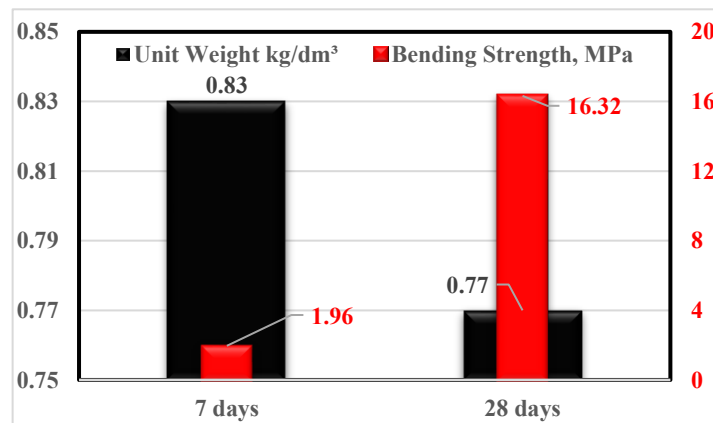
### 3. Results and Discussion

Figure 9 presents the unit weight and bending strength results of the samples. When examining the unit weight results, it is observed that the unit weight of the samples decreased from  $0.83 \text{ kg/dm}^3$  at 7 days to  $0.77 \text{ kg/dm}^3$  at 28 days. This corresponds to an approximate reduction of 7.2%. This decrease is likely due to the evaporation of moisture from the porous 3D textile structure and the waterproof membrane over time, leading to drying of the system. Although the use of a table vibrator during production ensured thorough dispersion of the cement paste into the textile structure, the overall porosity of the composite remained high. During the curing process, water loss occurred primarily through the open-pore upper surface, and this evaporation caused a reduction in mass. Additionally, some physically bound water may have been released from the system during the formation of hydration products and the microstructural development within the cementitious matrix, contributing to the observed weight loss.

In terms of bending strength, the value increased significantly from 1.96 MPa at 7 days to 16.32 MPa at 28 days, representing an approximate increase of 733%. This remarkable improvement can be attributed to the high early strength performance of white cement, as well as the improved mechanical interlocking between the 3D textile and the cementitious matrix over time. At early ages (7 days), the hydration products may not have sufficiently bonded to the textile fibers. However, by 28 days, the formation of a denser and more continuous C-S-H gel around the fibers significantly enhanced the interface, allowing the composite to carry higher loads under flexural stress. Furthermore, the adhesion of the waterproof membrane to the bottom surface of the samples likely contributed to the resistance against tensile forces generated during bending loading, limiting crack propagation and enhancing the overall bending strength.

This composite system, which exhibits low density but high bending strength, demonstrates the potential to meet both aesthetic and structural demands in architectural applications. Unlike conventional concrete materials, the

developed composite clearly benefits from the integration of textile reinforcement and waterproof membrane, providing a unique balance of lightness and mechanical performance.



**Figure 9.** Unit weight and bending strength of 3D Textile composite specimens

The remarkable increase in flexural strength between 7 and 28 days can primarily be attributed to the continuous hydration process of white cement, which is known for its high early strength but also continues to develop a denser microstructure over time. At 7 days, although initial hydration products had formed, the bonding between the cementitious matrix and the 3D textile fibers was still relatively weak, limiting load transfer capacity. By 28 days, the formation of a more cohesive and compact C–S–H gel significantly enhanced the fiber–matrix interface, enabling more efficient stress distribution under bending. Additionally, the waterproof membrane contributed to crack control in the tension zone during flexural loading, preventing premature failure and further improving the strength. This combination of improved interfacial adhesion, densification of the matrix, and reinforcement synergy explains the substantial strength gain observed at 28 days compared to 7 days.



**Figure 10.** Specimen appearances before the bending test

Figure 10 shows the general appearance of the specimens before the bending test, while Figure 11 presents the deformed state of the specimens after the test.

As seen in Figure 11, the specimens were able to bend up to approximately 6 cm without breaking. This clearly demonstrates the exceptional ductility and deformation capacity of the developed white cement-based textile-reinforced composite under bending loading. While conventional cementitious systems typically exhibit brittle fracture behavior, the specimens produced in this study withstood significant deformation without failure. The 3D textile structure likely played a critical role in this performance by absorbing tensile stresses during bending and delaying crack propagation, thus allowing for greater shape adaptation. Additionally, the waterproof membrane applied to the bottom surface of the specimen contributed to tensile resistance in the tension zone during bending, further enhancing the deformation capacity. A deflection of nearly 6 cm is a highly successful

result for such thin, lightweight composite systems and strongly indicates that the material is suitable for use in flexible and high-performance architectural applications.



**Figure 11.** Specimen appearances after the bending test

Figure 12 presents the dynamic and static tensile strength results of the specimens. Tensile tests were conducted under both rapid (dynamic) and slow (static) loading conditions, and results at 7 and 28 days were compared. At 7 days, the dynamic tensile strength was measured as 17.22 MPa, while the static tensile strength was 16.94 MPa. By 28 days, the dynamic strength increased to 17.82 MPa and the static strength to 17.52 MPa. These values show an approximate increase of 3.5% over time, which can be attributed to the continued hydration reactions in the cement matrix leading to a stronger fiber–matrix interface. Given the high early strength characteristics of white cement, the elevated tensile strengths observed even at early ages clearly reflect its positive contribution to mechanical performance.

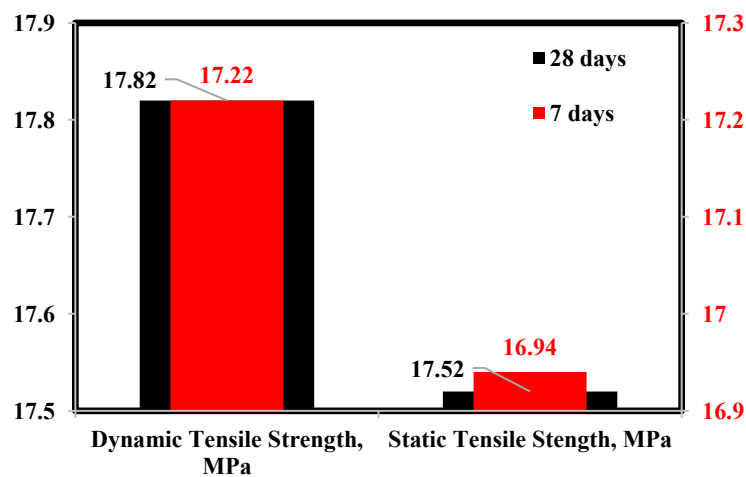


**Figure 12.** Tensile strength of 3D Textile composite specimens

When comparing dynamic and static loading conditions, it is evident that the dynamic tensile strength is slightly higher than the static tensile strength at both ages. The difference is approximately 1.6% at 7 days and 1.7% at 28 days. This small variation indicates that the composite responds similarly under both fast and slow loading, demonstrating effective resistance to both sudden and sustained stresses. Thanks to the embedded 3D textile reinforcement, the system maintained a high capacity to absorb and distribute energy even under rapid loading, while in static conditions, the textile structure sustained loads over a longer period without failure. This consistency confirms that the textile-reinforced matrix provides both strength and stable energy dissipation.

Overall, the concentration of both dynamic and static tensile strengths around 17 MPa represents a remarkably high performance for a thin and lightweight composite system. These results indicate that the material is not only suitable for shaping and architectural formwork but also possesses the structural integrity and load-bearing capacity required for broader applications. Additionally, its ability to perform consistently under both dynamic and static loads makes it a promising candidate for use in applications where sudden forces, such as seismic activity, might occur.

From an architectural perspective, the material's strong and stable performance under both dynamic and static tensile conditions offers significant advantages—especially for non-load-bearing elements that still require deformation capacity and stress transfer. For instance, in curved surfaces, free-form façade elements, or flexible temporary structures, this type of composite provides both aesthetic freedom and mechanical reliability. Its resistance to sudden loads ensures shape retention under wind suction, impact, or user-induced forces, making it a durable and appealing component for contemporary architectural designs.

Figure 13 shows the appearance of the specimens during the tensile test. A striking observation in Figure 13 is that during the tensile loading, the cementitious matrix begins to crumble and fragment under increasing stress; however, the overall integrity of the specimen remains intact due to the embedded 3D textile reinforcement. This behavior highlights the critical role of the textile in bridging cracks and maintaining structural continuity even after the brittle failure of the cement paste. While traditional cement-based materials typically fail catastrophically under tension, the presence of the textile grid allows the composite to redistribute stresses and delay complete separation. This crack-bridging mechanism not only enhances the material's ductility but also provides a form of post-cracking load transfer, which is essential for both structural resilience and safety. Such behavior is particularly valuable in architectural applications where deformation without disintegration is necessary for maintaining aesthetic and functional performance under stress.



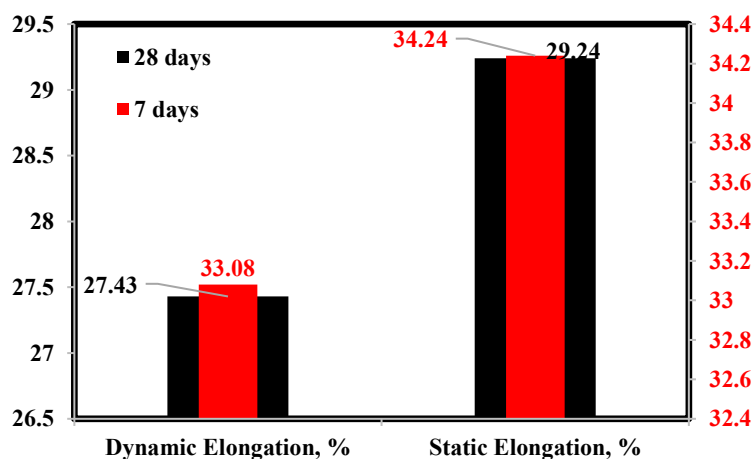
**Figure 13.** Appearance of the specimen during the tensile test

Figure 14 presents the dynamic and static tensile elongation values of the specimens. According to the test results, the specimens exhibited remarkably high tensile elongation under both dynamic and static loading conditions. At 7 days, dynamic tensile elongation was measured as 33.08%, while static elongation was slightly higher at 34.24%. By 28 days, these values decreased to 27.43% and 29.24%, respectively. This reduction, approximately

17%, can be attributed to the progressive hardening of the cementitious matrix over time. As hydration reactions advance, the matrix becomes denser and more crystalline, reducing the composite's overall ductility and limiting its elongation capacity. Considering the high early strength development of white cement, the greater elongation observed at 7 days suggests that during early curing, the matrix had not yet fully stiffened, allowing the textile to carry more of the load and enabling the system to behave more flexibly.

When comparing dynamic and static tensile elongation, it is evident that static elongation is slightly higher at both ages. This difference is approximately 3.5% at 7 days and 6.6% at 28 days. The slower rate of loading in static conditions likely allows the textile fibers to deform more gradually and uniformly, maximizing their elongation potential. In contrast, under dynamic loading, the rapid application of force results in a shorter deformation time, limiting the overall elongation despite the material's inherent energy absorption capacity. Nevertheless, in both conditions, elongation values exceeding 25% clearly indicate that the textile-reinforced composite is highly ductile and capable of sustaining significant deformation without failure.

In conclusion, these high elongation values demonstrate that the material performs exceptionally well not only in terms of tensile strength but also in flexibility and deformation capacity. This makes it highly suitable for architectural applications where curvature, bendability, or form retention under stress is essential—such as in freeform surfaces, foldable structural components, or stress-adaptive façade systems.



**Figure 14.** Elongation of 3D Textile composite specimens

Figure 15 shows the elongation and fracture zones of the specimen after the tensile test. As observed in Figure 15, the specimen undergoes noticeable elongation under tensile loading, yet maintains its structural integrity throughout the deformation process. This indicates that the embedded 3D textile acts as a reinforcing skeleton—bridging cracks, carrying tensile stresses, and effectively distributing energy across the composite. Although microcracking occurs in the cement matrix during elongation, the textile prevents the specimen from disintegrating, ensuring overall cohesion until failure. At the point of fracture, it is clearly seen that the break occurs primarily between the gripping jaws, precisely where the tensile stress is most concentrated. This localized failure suggests a mechanically consistent behavior, reinforcing the reliability of the test.

Additionally, despite the significant elongation observed during testing, there is no excessive or uncontrolled deformation at the point of failure. This reveals that the composite exhibits a controlled fracture mechanism—breaking progressively rather than catastrophically. Such behavior is particularly valuable in architectural applications where both safety and aesthetics are important. The ability to undergo substantial strain while maintaining form and cohesion makes this material a strong candidate for use in adaptive or deformable architectural components.

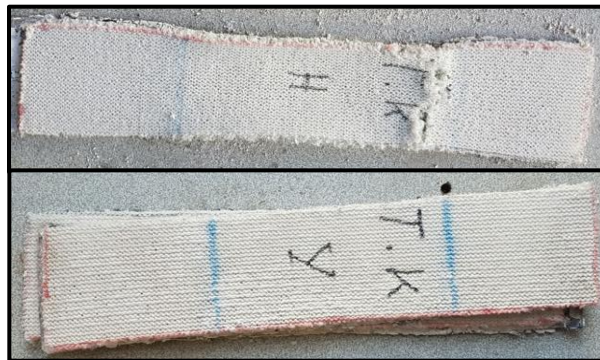


**Figure 15.** Elongation and fracture of the specimen after the tensile test

Figure 16 presents the stress–strain curves obtained from static and dynamic tensile tests at 7 and 28 days. The stress–strain curves reveal that all specimens exhibited remarkably high deformation capacities, though their behavior varied depending on age and loading type. In the 7-day static test, the tensile stress peaked at 16.94 MPa with a corresponding strain of 34.24%. In comparison, the 7-day dynamic test reached a slightly higher stress of 17.22 MPa at a strain of 33.08%. These results indicate that the textile reinforcement effectively limited crack propagation in both loading types at early ages, allowing for significant deformation before failure. Notably, in the 7-day dynamic test, the material experienced rapid deformation even at relatively low stress levels—reaching 10% strain much earlier—indicating that the fibers underwent faster elongation under rapid loading conditions.

At 28 days, the static test showed a maximum stress of 17.52 MPa with a strain of 29.24%, while the dynamic test reached 17.82 MPa with a slightly lower strain of 27.43%. These results show that over time, the cement matrix becomes stiffer and more resistant, leading to a decrease in overall strain capacity but a slight increase in tensile strength. In the 28-day dynamic loading scenario, the system achieved higher stress levels at lower strain values, which suggests improved fiber–matrix interaction and more efficient stress transfer due to ongoing hydration and matrix densification.

When comparing all test conditions, it becomes evident that static loading results in slower, more controlled deformation, enabling higher overall strain values. In contrast, dynamic loading accelerates the deformation process but results in slightly lower total strain. Despite this, the curves in all cases indicate that the material can absorb substantial stress and strain before failure, demonstrating a highly ductile behavior. Strain values exceeding 25%—particularly in such thin composite sections—are uncommon and highlight the material's ability to maintain form under tensile forces, absorb energy efficiently, and resist brittle failure, which is essential for architectural applications requiring both flexibility and durability.

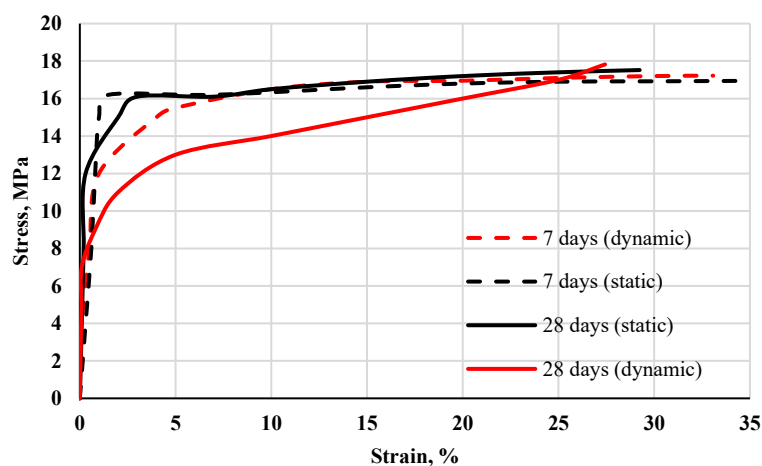


**Figure 16.** Stress-strain curve of 3D Textile composite specimens

## 4. Conclusion

The following results were obtained from this study:

- The developed textile-reinforced thin-section cementitious composites exhibited remarkably low unit weights (0.77–0.83 kg/dm<sup>3</sup>) while achieving high flexural strength (16.32 MPa). This demonstrates a significant advantage for producing lightweight structural elements that offer both load-bearing capacity and design flexibility.
- The specimens maintained structural integrity up to failure under both static and dynamic tensile loading conditions, showing high deformation capacity. This indicates that the textile reinforcement limited crack propagation, enhanced load-bearing performance, and contributed to energy absorption capacity.
- Stress–strain curves revealed that the specimens could undergo more than 30% elongation. These exceptionally high values for such thin-section, cement-based materials prove that the composite is ductile, shape-adaptive, and highly resistant to deformation.
- The results suggest that this composite system is suitable for architectural applications such as freeform, flexible, foldable, or rollable structural elements. Its low weight and water resistance also make it ideal for portable, temporary, or special-purpose architectural structures.
- Observations during the tensile test showed that although the cement matrix started to crumble initially, the textile reinforcement preserved the integrity of the specimen. This proves that the textile acts not only as a strength-enhancing component but also as a unifying and crack-bridging element.

The promising results obtained in this study demonstrate that 3D textile-reinforced white cement-based composites hold significant potential for architectural applications. Future research is expected to enhance mechanical performance by exploring different textile layer configurations, including multilayered and directionally oriented placements. Furthermore, the long-term durability of the material under environmental factors such as UV exposure, humidity, and temperature variations should be assessed. Additionally, investigating the printability and interlayer bonding of this composite will facilitate its integration with digital fabrication technologies.

## Acknowledgements

This study was not funded by any organization.

## Declaration of Competing Interest

The authors declare that they have no known competing financial interests or personal relationships that could have appeared to influence the work reported in this paper.

## Authorship Contribution Statement

**Serdal Ünal:** Conceptualization, Methodology, Writing - original draft preparation

**Kerem Aybar:** Formal analysis and investigation

**Ömer Karagöz:** Writing - review and editing

**Mehmet Canbaz:** Supervision

## References

- [1] C. Wu, Y. Pan, L. Yan, "Mechanical properties and durability of textile reinforced concrete (TRC)—a review," *Polymers*, vol. 15, no.18, 3826, Sep. 2023, doi:10.3390/polym15183826.
- [2] N. K. Barman, S. S. Bhattacharya, R. Alagirusamy, "Textile structures in concrete reinforcement," *Text. Prog.*, vol.56, no.1, pp. 1-229, Jan 2024, doi: 10.1080/00405167.2023.2266930.
- [3] M. Raupach, C. M. Cruz, "Textile-reinforced concrete: Selected case studies," in *Textile Fibre Composites in Civil Engineering*, Woodhead Publishing Series in Civil and Structural Engineering, 2016, pp. 275-299.
- [4] S. G. Venigalla, A. B. Nabilah, N. A. Mohd Nasir, N. A. Safiee, F. N. A. Abd Aziz, "Textile-reinforced concrete as a structural member: a review," *Buildings*, vol. 12, no.4, 474, Apr. 2022, doi: 10.3390/buildings12040474.

- [5] P. Valeri, P. Guaita, R. Baur, M. Fernández Ruiz, D. Fernández-Ordóñez, A. Muttoni, "Textile reinforced concrete for sustainable structures: Future perspectives and application to a prototype pavilion," *Struct. Concr.*, vol.21, no.6, pp. 2251-2267, Dec. 2020, doi: 10.1002/suco.201900511.
- [6] S. Liu, X. Ma, Y. Ma, Z. Chen, Z. Dong, P. Ma, "Review on the design and application of concrete canvas reinforced with spacer fabric," *J. Eng. Fibers Fabr.*, vol. 18, 15589250231152591, Mar. 2023, doi:10.1177/15589250231152591.
- [7] Z. Jun., X. Wei, W. Xingzhong, "Application and research status of concrete canvas and its application prospect in emergency engineering," *J. Eng. Fibers Fabr.*, vol.15, 1558925020975759, Nov. 2020, doi:10.1177/1558925020975759.
- [8] N. S. Karaduman, Y. Karaduman, H. Ozdemir, G. Ozdemir, "Textile reinforced structural composites for advanced applications," in *Textiles for Advanced Applications*, IntechOpen. 2017, ch. 4, pp.87-113.
- [9] M. Zhang, M. Deng, "Tensile behavior of textile-reinforced composites made of highly ductile fiber-reinforced concrete and carbon textiles," *J. Build. Eng.*, vol. 57, 104824, Oct. 2022, doi: 10.1016/j.jobbe.2022.104824.
- [10] K. Kong, Z. Mesticou, M. Michel, A. S. Larbi, A. Junes, "Comparative characterization of the durability behaviour of textile-reinforced concrete (TRC) under tension and bending," *Compos. Struct.*, vol. 179, pp. 107-123, Nov. 2017, doi: 10.1016/j.compstruct.2017.07.030.
- [11] M. El Kadi, P. Kapsalis, D. Van Hemelrijck, J. Wastiels, T. Tysmans, "Influence of loading orientation and knitted versus woven transversal connections in 3D textile reinforced cement (TRC) composites," *Appl. Sci.*, vol. 10, no.13, 4517, Jul. 2020, doi:10.3390/app10134517.
- [12] D. Friese, M. Scheurer, L. Hahn, T. Gries, C. Cherif, "Textile reinforcement structures for concrete construction applications—a review," *J. Compos. Mater.*, vol. 56, no.26, pp. 4041-4064, Nov. 2022, doi:10.1177/00219983221127181.
- [13] V. Rubeziene, S. Varnaite, J. Baltusnikaite, I. Padleckiene, "Effects of light exposure on textile durability," in *Understanding and Improving the Durability of Textiles*, Woodhead Publishing, Oxford, 2012, pp.104-125.
- [14] S. Yin, L. Jing, M. Yin, B. Wang, "Mechanical properties of textile reinforced concrete under chloride wet-dry and freeze-thaw cycle environments," *Cem. Concr. Compos.*, vol. 96, pp. 118-127. Feb. 2019, doi: 10.1016/j.cemconcomp.2018.11.020.
- [15] J. Hill, "Rolling out the Concrete." Accessed: May 21, 2023. [Online.] Available: <https://www.world-architects.com/en/architecture-news/film/rolling-out-the-concrete>.
- [16] N. Williams Portal, K. Lundgren, H. Wallbaum, K. Malaga, "Sustainable potential of textile-reinforced concrete," *J. Mater. Civ.*, vol. 27, no.7, 04014207, Jul. 2015, doi: 10.1061/(ASCE)MT.1943-5533.0001160.
- [17] Y. Tarhan, İ. H. Tarhan, Y. Jacquet, A. Perrot, "Mechanical behaviour of 3D printed and textile-reinforced eco-friendly composites," *J. Sustain. Cem.-Based Mater.*, vol.14, no.3, pp. 477-495, Mar.2025. doi: 10.1080/21650373.2024.2396420.
- [18] F. Y. Han, H. S. Chen, X. Li, B. Bao, T. Lv, W. Zhang, D. W. Hui, "Improvement of mechanical properties of concrete canvas by anhydrite-modified calcium sulfoaluminate cement," *J. Compos. Mater.*, vol. 50, no.14, pp. 1937-1950, Jun. 2016, doi:10.1177/0021998315597743.
- [19] F. Y. Han, H. S. Chen, W. L. Zhang, T. Lv, Y. J. Yang, "Influence of 3D spacer fabric on drying shrinkage of concrete canvas," *J. Ind. Text.*, vol. 45, no. 6, pp. 1457-1476, May 2016, doi:10.1177/1528083714562087.